

# Direct Growth of ZnO Nanocrystals onto the Surface of Porous TiO<sub>2</sub> Nanotube Arrays for Highly Efficient and Recyclable Photocatalysts\*\*

Hui Ying Yang, Siu Fung Yu,\* Shu Ping Lau, Xiwang Zhang, Darren Delai Sun, and Guo Jun

Recently, extensive investigations have been concentrated on the design and synthesis of nanocomposite metal oxides such as ZnO/TiO<sub>2</sub> nanocomposite materials to improve the quantum efficiency of photocatalysts for applications in water purification.<sup>[1–3]</sup> This is due to the high reactivity of TiO<sub>2</sub> and the large binding energy of ZnO, which improve the process of electron and hole transfer between the corresponding conduction and valence bands. As a result, a better separation of photo-generated carriers can be achieved when compared with catalysts from a single metal oxide.<sup>[3]</sup>

A double-layered ZnO/TiO<sub>2</sub> system had been proposed to improve the quantum efficiency of photocatalysts, however, the photogenerated electrons accumulated in the TiO<sub>2</sub> underlayer may be unavailable to participate in the photocatalytic reactions so that the corresponding quantum efficiency could be degraded.<sup>[4,5]</sup> ZnO tetrapods coated with TiO<sub>2</sub> nanoparticles were also suggested for the realization of high efficiency photocatalysts,<sup>[1]</sup> but the poor control of the total surface exposure area for both metal oxides limited their usefulness as high efficiency photocatalysts. Alternatively, the use of a

suspended TiO<sub>2</sub> and ZnO nanopowder mixture demonstrated highly effective photocatalytic reactions.<sup>[2]</sup> In addition, the realization of bicomponent nanofiber photocatalysts can achieve large surface exposure areas of both components as well as highly effective photocatalytic reactions.<sup>[4]</sup> Unfortunately, the separation of these semiconductor nanocrystals/nanofibers from the treated water is very difficult and energy-consuming so that their usefulness is limited in practical applications.<sup>[6–8]</sup> So far there are no highly efficient nanocomposite photocatalysts that can achieve a large surface exposure area, are easy to handle and recyclable, and are suitable for practical applications.

In this paper, we propose the use of ZnO nanocrystal-coated, vertically oriented, porous TiO<sub>2</sub> nanotube arrays for efficient and low-cost photocatalysts. The advantages of the proposed composite nanostructures are as follows. The exposed surface area of the ZnO nanocrystals onto the porous TiO<sub>2</sub> nanotubes and the contact area between ZnO and TiO<sub>2</sub> (i.e., the area of the ZnO/TiO<sub>2</sub> interfaces) can be maximized to achieve highly efficient photocatalytic decomposition via heterojunction effect. The configuration of vertically aligned nanotube arrays also allows the diffusion of reactants through multiple pathways to enhance light harvest. Furthermore, the formation of composite nanotube arrays on bulk Ti film allows easy recovery of photocatalysts. Therefore, the resulting composite nanostructures may be an attractive photocatalyst for environmental purification.

Figure 1 shows the structure and surface morphology of the porous TiO<sub>2</sub> nanotubes. The scanning electron microscopy (SEM) image in Figure 1a shows that the porous TiO<sub>2</sub> nanotubes have an average length and diameter of 3.5 μm and 120 nm, respectively. Figure 1b shows the transmission electron microscopy (TEM) image that confirms the formation of grains and voids of a single porous TiO<sub>2</sub> nanotube. In addition, the porous TiO<sub>2</sub> nanotubes show no inner-tube structure after the thermal annealing process. The corresponding high-resolution TEM (HRTEM) image was recorded and the typical results are shown in Figure 1c. The lattice spacing is found to be 3.52 Å, which is associated with the (101) interplanar distance of anatase TiO<sub>2</sub> (see the inset fast Fourier transform (FFT) patterns). The energy dispersive X-ray (EDX) data is also shown in Figure 1d, where the local composition of the selected regions of the nanotubes given in Figure 1b is

[\*] Prof. S. F. Yu, Dr. H. Y. Yang  
School of Electrical & Electronic Engineering  
Nanyang Technological University  
Singapore 639798 (Singapore)  
E-mail: esfyu@ntu.edu.sg

Prof. S. P. Lau  
Department of Applied Physics  
The Hong Kong Polytechnic University  
Hung Hom, Kowloon, Hong Kong (P. R. China)

Dr. X. Zhang, Prof. D. D. Sun  
School of Civil & Environment Engineering  
Nanyang Technological University  
Singapore 639798 (Singapore)

G. Jun  
School of Material Science & Engineering  
Nanyang Technological University  
Singapore 639798 (Singapore)

[\*\*] The authors acknowledge a LKY PDF 2/08 start up grant for the support of this research.

Supporting Information is available on the WWW under <http://www.small-journal.com> or from the author.

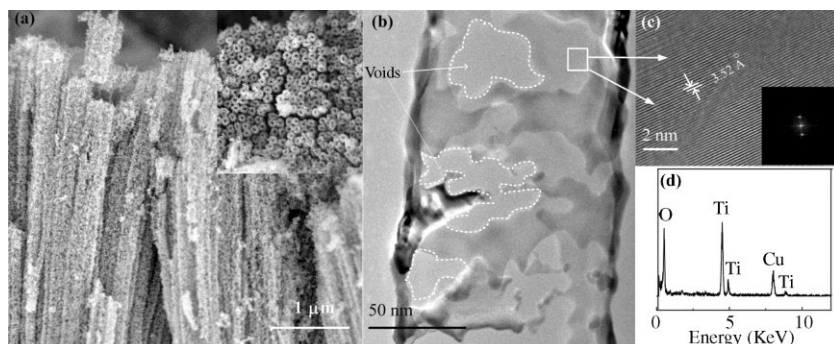


**Figure 1.** a) Cross-sectional SEM images of the porous TiO<sub>2</sub> nanotubes fabricated by electrochemical anodization. The inset shows the surface SEM image of the TiO<sub>2</sub> nanotubes. b) TEM image of a single TiO<sub>2</sub> nanotube. c) HRTEM image of the TiO<sub>2</sub> nanotube. The inset shows the corresponding FFT diffraction patterns (FFT-DP). d) EDX spectra collected from the stems of the TiO<sub>2</sub> nanotubes.

analyzed. It is observed from the EDX analysis that titanium and oxygen are the dominant elements presented in the porous TiO<sub>2</sub> nanotubes.

Typical SEM images of the porous TiO<sub>2</sub> nanotubes with attached ZnO nanocrystals are shown in Figure 2a. The average diameter of the ZnO/TiO<sub>2</sub> composite nanotubes was ≈180 nm and the length remained 3.5 μm. The outer wall of the porous TiO<sub>2</sub> nanotubes is completely coated with ZnO nanocrystals.

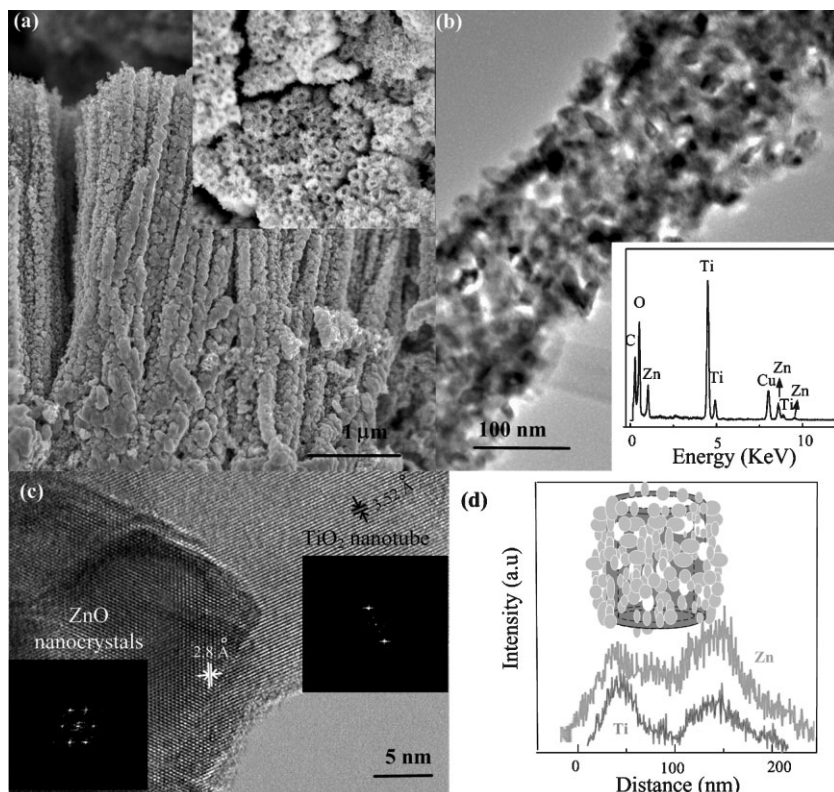


**Figure 2.** a) Cross-sectional SEM images of the porous TiO<sub>2</sub> nanotubes covered with ZnO nanocrystals. The inset shows the corresponding surface SEM image. b) TEM image of a single TiO<sub>2</sub> nanotube covered with ZnO nanocrystals. The inset shows the EDX spectra collected from the stem of the nanotubes. c) HRTEM image of the interface between ZnO nanocrystals and porous TiO<sub>2</sub> nanotubes. The insets show the corresponding FFT-DP. d) Content analysis of the ZnO/TiO<sub>2</sub> composite nanotubes by scanning TEM.

Although the flow direction of the ZnO plasma is parallel to the length of the nanotubes, the inner tube of the ZnO/TiO<sub>2</sub> composite nanotubes is only slightly filled with the ZnO nanocrystals. Figure 2b shows a low-magnification TEM image of a single composite nanotube. The ZnO nanocrystals, which have average diameter of ≈30 nm, were grown uniformly around the surface of the TiO<sub>2</sub> nanotube. The inset of Figure 2b shows the chemical analysis of the composite nanotubes by EDX analysis. From the EDX results, it can be observed that the dominant elements in the composite nanotubes are titanium, zinc, and oxygen. A HRTEM image and FFT patterns of the interface between TiO<sub>2</sub> and ZnO is shown in Figure 2c, revealing that TiO<sub>2</sub> and ZnO are

of anatase and wurtzite crystal structures, respectively. A distinct boundary is visible and no transitional layer is found. This indicated that the ZnO nanocrystals were fused together with a TiO<sub>2</sub> nanotube to form a single structure in the deposition process. The spatial distributions of the atomic composition across the composite nanotube were detected by a nanoprobe EDX line-scan analysis. As shown in Figure 2d, the TiO<sub>2</sub> nanotube was homogeneously coated with ZnO nanocrystals.

Figure 3 shows the X-ray diffraction (XRD) results of the entire ZnO/TiO<sub>2</sub> composite nanotubes. Most of the diffraction peaks of the composite nanotubes are perfectly indexed to the anatase TiO<sub>2</sub> phases (JCPDS file No. 21-1272), however, diffraction peaks related to rutile TiO<sub>2</sub> phases are too weak to be observed from the XRD pattern. The remaining peaks are connected to wurtzite ZnO (JCPDS file No. 36-1451). It can be concluded that the anatase TiO<sub>2</sub> and wurtzite ZnO are the dominant phases in the ZnO/TiO<sub>2</sub> composite nanotubes. Furthermore, the XRD peaks of the TiO<sub>2</sub> portion of the composite nanotubes do not shift when compared with those of the pure TiO<sub>2</sub> nanostructures. This indicates that the Zn element does not substitute into the TiO<sub>2</sub> lattices for Ti and that there is no formation of solid solution.

The photocatalytic activities of the ZnO/TiO<sub>2</sub> composite nanotubes were evaluated by studying the photocatalytic degradation of humic acid (HA), which is a major health risk to natural organic matter in surface water and ground water.<sup>[9,10]</sup> The photocatalytic degradation characteristics of HA by TiO<sub>2</sub> nanotubes and ZnO nanorods, which have similar diameters and lengths to that of the ZnO/TiO<sub>2</sub> composite nanotubes, were also studied. Hence, the influence of heterojunction effects on the improvement

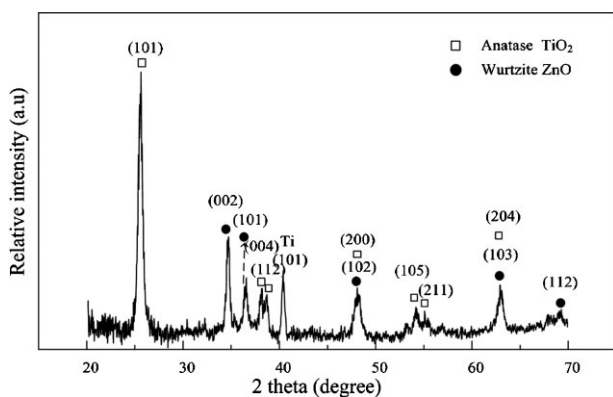


Figure 3. XRD pattern of the ZnO/TiO<sub>2</sub> composite nanotubes.

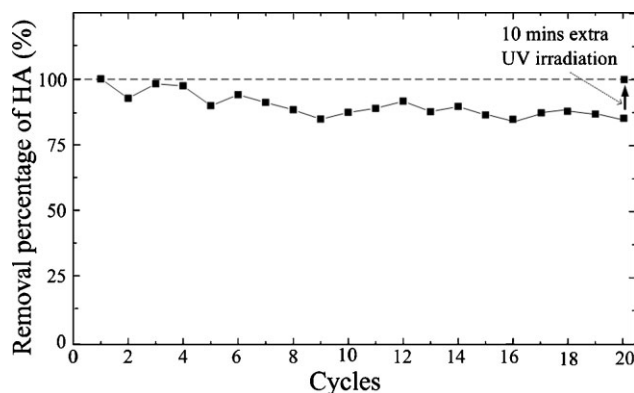


Figure 5. The recyclability test of the photocatalytic decomposition rate of HA for the ZnO/TiO<sub>2</sub> composite nanotubes.

of photocatalytic decomposition of the composite nanotubes can be studied. The pure ZnO nanorods were fabricated by the hydrothermal method and the corresponding fabrication process can be found in Reference [11].

All the samples with size 1 cm × 2.5 cm were soaked into four identical bottles containing HA (50 mg L<sup>-1</sup>, 10 mL) and stored in a dark environment for 30 min to reach adsorption equilibrium of HA before exposure to UV light (254 nm, 8 W) at room temperature. All the bottles were placed 5 cm away from the UV light with the nanostructures facing the UV light in order to ensure that all the photocatalysts should receive the same amount of UV radiation. The bottles containing blank HA solution, porous TiO<sub>2</sub> nanotubes, ZnO nanorods, and ZnO/TiO<sub>2</sub> composite nanotubes were labeled as sample 1, 2, 3, and 4, respectively. HA concentration of the sample at different intervals was monitored by measuring the absorbance at 436 nm on a UV/Vis spectrophotometer (UV-1700 Shimadzu). Figure 4 compares the HA decomposition rate of all the samples over a period of time. After 65 min of photocatalytic reaction, 55%, 80%, and 100% of HA concentration was

removed by sample 2, 3, and 4, respectively. The inset photo was taken after 65 min of reaction. It is obvious that the ZnO/TiO<sub>2</sub> composite nanotubes exhibited a much higher photocatalytic activity than that of the pure ZnO nanorods or pure TiO<sub>2</sub> nanotubes. The photocatalytic degradation of HA in bottle 1 to 4 followed zero-order kinetics and the reaction rate constant  $k$  of HA degradation for sample 4 was 0.015 min<sup>-1</sup>, which was more than ≈1.4 times that of sample 3 (0.011 min<sup>-1</sup>) and ≈2 times that of sample 2 (0.007 min<sup>-1</sup>).

Figure 5 plots the photodegradation percentages of HA concentration by sample 4 for repeat use in the photocatalytic process (i.e., in each process cycle, the same sample was placed into a fresh bottle of HA for 65 min of UV illumination). The ZnO/TiO<sub>2</sub> composite nanotubes showed no apparent change in surface morphology after 20 cycles of reuse. In addition, the photodegradation percentage of HA was only slightly reduced by 10%, which can be recovered by 10 min of extra exposure to the UV light. This indicated that the ZnO/TiO<sub>2</sub> composite nanotubes are very stable in physical strength and chemical properties.

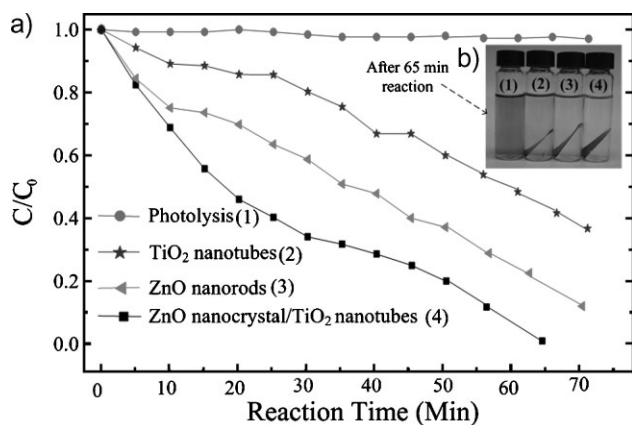
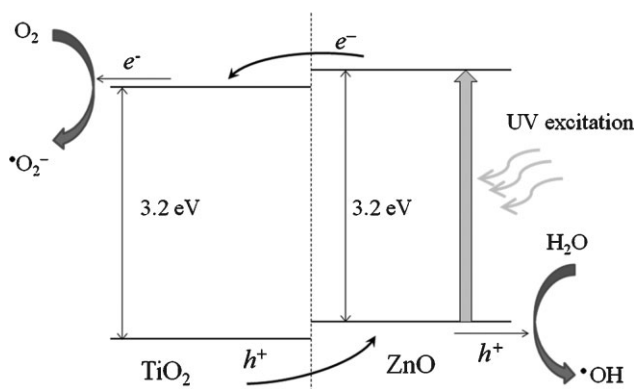


Figure 4. a) Comparison of photocatalytic decomposition rates of HA of 1) reference HA solution, 2) TiO<sub>2</sub> nanotubes, 3) ZnO nanorods, and 4) ZnO/TiO<sub>2</sub> composite nanotubes. b) The photograph of HA after 65 min of photocatalytic decomposition by the four samples.

The purpose of having pores on the TiO<sub>2</sub> nanotubes is to limit the available area of surface contact so that ZnO nanocrystals can be formed instead of the deposition of a ZnO thin film. The surface area of the ZnO/TiO<sub>2</sub> composite nanotubes coated with ZnO nanocrystals can be 1.5 times larger than that deposited with the same thickness of ZnO thin film.<sup>[12]</sup> Furthermore, about 80% of the surface area of the porous TiO<sub>2</sub> nanotubes form heterojunctions with the ZnO nanocrystals.<sup>[13]</sup> It must be noted that 100% coverage can be realized by coating the nanotubes with a layer of a ZnO thin film. Hence, this verified that the use of ZnO nanocrystals can increase the surface area of the composite nanotubes as well as maintain a large contact area to favor a heterojunction effect.

The principle of photocatalytic decomposition via ZnO/TiO<sub>2</sub> heterojunctions is shown in Figure 6. Electrons transfer from the ZnO conduction band to the TiO<sub>2</sub> conduction band and conversely, holes transfer from the TiO<sub>2</sub> valence band to the ZnO valence band under UV excitation. Due to the presence of a ZnO/TiO<sub>2</sub> heterojunction (i.e., potential barrier), the chance for the recombination of electron–hole pairs will be



**Figure 6.** Schematic band diagram representing the charge-transfer process in the ZnO/TiO<sub>2</sub> composite. Electrons ( $e^-$ ) and holes ( $h^+$ ) migrate to the surface of TiO<sub>2</sub> and ZnO, respectively, after photon excitation by UV illumination and react with the adsorbed species. The species will then be decomposed by HO $\cdot$  and  $\cdot\text{O}_2^-$  radicals.

reduced. This increases the availability of the electrons (holes) to migrate to the TiO<sub>2</sub> (ZnO) surface of the ZnO/TiO<sub>2</sub> composite photocatalysts and consequently improves the occurrence of redox processes—electrons reduce dissolved molecular oxygen to superoxide  $\cdot\text{O}_2^-$  radical anions while holes form hydroxyl radicals, HO $\cdot$ . Organic molecules present in the solution will then react with these oxidizing agents to induce oxidative degradation to inorganic compounds including CO<sub>2</sub> and H<sub>2</sub>O. The reaction rate constant  $k$  increases by 2 times if TiO<sub>2</sub> nanotubes are replaced by ZnO/TiO<sub>2</sub> composite nanotubes as the photocatalyst (Figure 4). As the increase of  $k$  is larger than the increase of surface area, it is believed that the combined effects of a large surface area and heterojunctions lead to the improvement of photoactivity.

In conclusion, we have shown that the ZnO/TiO<sub>2</sub> composite nanotubes have excellent photocatalytic activities for the decomposition of HA when compared with the performance of pure ZnO nanorods and TiO<sub>2</sub> nanotubes. This is because i) the composite nanotubes can allow both metal oxides to have a large surface exposure area to the surroundings, and ii) the heterojunction structure can promote an increase in the charge separation of the photogenerated electrons and holes within the composite nanostructures to enhance photocatalytic reaction. This novel photocatalyst can achieve high quantum efficiency and lead to high photocatalytic activity. Furthermore, it has been shown that the bulky size of the proposed photocatalysts can be easily recovered and their robustness to the environment allows them to be reused. Therefore, the proposed technique to synthesize ZnO/TiO<sub>2</sub> composite nanotubes represents a significant advance for environmental applications.

## Experimental Section

The fabrication process of ZnO nanocrystals onto porous TiO<sub>2</sub> nanotube arrays can be realized by a simple three-step process as shown in Figure 7. i) Growth of a high-aspect-ratio, vertically aligned, single-wall TiO<sub>2</sub> nanotubular layer on Ti film by

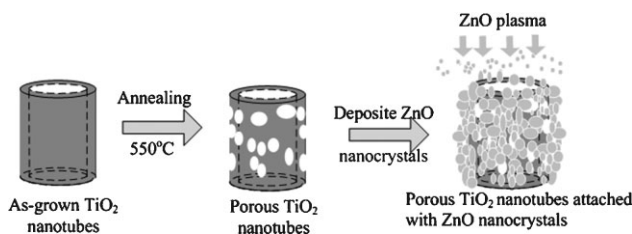


**Figure 7.** Fabrication process of the porous TiO<sub>2</sub> nanotubes with attached ZnO nanocrystals.

electrochemical anodization of Ti foil at room temperature. Detailed fabrication procedures of the TiO<sub>2</sub> nanotubes can be found in Reference [14]. ii) Formation of porous TiO<sub>2</sub> nanotubes by thermal annealing. During the thermal-annealing process, TiO<sub>2</sub> nanotubes were heated at 550 °C in an open air furnace for 3 h. This procedure allows the formation of grains and voids (as well as pores because the wall thickness of the nanotubes is  $\approx 20$  nm) along the TiO<sub>2</sub> nanotubes. iii) Growth of ZnO nanocrystals onto the surface of the porous TiO<sub>2</sub> nanotubes by room-temperature deposition of ZnO plasma using the filtered cathodic-vacuum-arc technique.<sup>[15]</sup>

The porous TiO<sub>2</sub> nanotubes were placed in the direction parallel to the flow direction of ZnO plasma. Hence, the rough surface of the nanotubes allows the capture and growth of ZnO nanocrystals. Only a few ZnO nanocrystals will be formed inside the TiO<sub>2</sub> nanotubes (i.e., the inner-tube surface). Different locations of TiO<sub>2</sub> nanotubes will experience different growth rates of ZnO nanocrystals. The surface where the excess deposition of ZnO plasma occurs will cause the pores to be covered with ZnO nanocrystals.

## Keywords:

nanocrystals · nanotubes · photocatalysis · titanium oxide · zinc oxide

- [1] Q. H. Zhang, G. W. Fan, L. Gao, *Appl. Catal. B* **2007**, *76*, 168.
- [2] G. Marci, V. Augugliaro, M. J. López-Muñoz, G. Martín, L. Palmisano, V. Rives, M. Schiavello, R. J. D. Tilley, A. M. Venezia, *J. Phys. Chem. B* **2001**, *105*, 1026.
- [3] D. Barreca, E. Comini, A. P. Ferrucci, A. Gasparotto, C. Maccato, C. Maragno, G. Sberveglieri, E. Tondello, *Chem. Mater.* **2007**, *19*, 5642.
- [4] Z. Liu, D. D. Sun, P. Guo, J. O. Leckie, *Nano Lett.* **2007**, *7*, 1081.
- [5] H. Y. Zhu, X. P. Gao, Y. Lan, D. X. Song, Y. X. Xi, J. C. Zhao, *J. Am. Chem. Soc.* **2004**, *126*, 8380.
- [6] K. Hashimoto, H. Iwata, A. Fujitshima, *Jpn. J. Appl. Phys.* **2005**, *44*, 8269.
- [7] E. S. Jang, J. H. Won, S. J. Hwang, J. H. Choy, *Adv. Mater.* **2006**, *18*, 3309.
- [8] Z. X. Li, F. B. Li, C. L. Yang, W. K. Ge, *J. Photochem. Photobiol. A* **2001**, *141*, 209.
- [9] C. S. Uyguner, M. Bekbolet, *Appl. Catal. B* **2004**, *49*, 267.
- [10] I. K. Konstantinou, T. A. Albanis, *Appl. Catal. B* **2004**, *49*, 1.
- [11] E. S. P. Leong, S. F. Yu, S. P. Lau, A. P. Abiyasa, *IEEE Photonics Technol. Lett.* **2007**, *19*, 1792.
- [12] If  $n$  identical ZnO hemispheres with diameter  $d$  are uniformly aligned (edge-to-edge) on the same horizontal surface of a TiO<sub>2</sub> nanotube with radius of  $r$  (i.e.,  $2\pi r \approx nd$ ), the total surface area of

all the ZnO hemispheres,  $A_{nc}$ , is  $A_{nc} = 2n\pi(d/2)^2$ . The surface area of the TiO<sub>2</sub> nanotubes covered by the ZnO thin film with thickness and width of  $d/2$  and  $d$ , respectively,  $A_{nt}$ , is  $A_{nt} = 2\pi(r + d/2)d$ . Using the approximation that  $d \approx r \sin(2\pi/n)$ , it can be shown that the maximum value of  $A_{nc}/A_{nt} \approx \pi/2$  if  $n$  is large and  $r \gg d/2$  (see also Supporting Information).

[13] If we wanted to cover a surface using circles with diameter  $d$ , the minimum surface of coverage will be  $(\pi d^2/4)/d^2 = \pi/4$  or 80%.

[14] J. M. Macak, M. Zlamal, J. Krysa, P. Schmuki, *Small* **2007**, *3*, 300.

[15] C. Yuen, S. F. Yu, S. P. Lau, C. K. Chen, *J. Crystal Growth* **2006**, *287*, 204.

Received: May 1, 2009

Revised: May 28, 2009

Published online: July 6, 2009